



Study on the 3DVar emission inversion method combined with machine learning in CMAQ

Reporter: Congwu Huang

Congwu Huang, Tijian Wang, Tao Niu

Hubei University

Nanjing University

Chinese Academy of Meteorological Sciences





Contents

- Introduction
- Data and Methods
- Results
- Conclusion



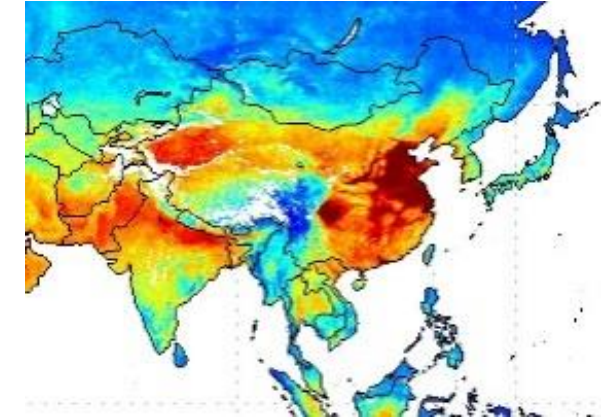
Major sources of uncertainty in air quality models

Initial and Boundary conditions

- global distribution
- nested simulation results
- previous simulation results

Emissions

- anthropogenic emissions
- natural emissions

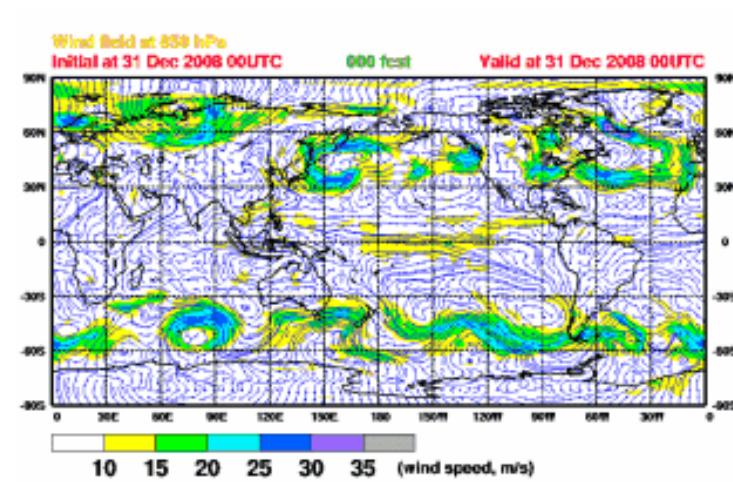


Meteorology

- Clouds
- Wind, temperature, humidity, pressure
- Planetary boundary layer height, local circulations

Processes

- chemistry
- dry deposition



Constantinescu et al., 2007a,2007b; Bocquet et al., 2015



Emission inversion

- 4DVAR and EnKF are two main methods that usually used to adjust emissions.
- Nudging is a relatively simpler method in emission data assimilation, but it can not deal with nonlinear problem or lack of observation

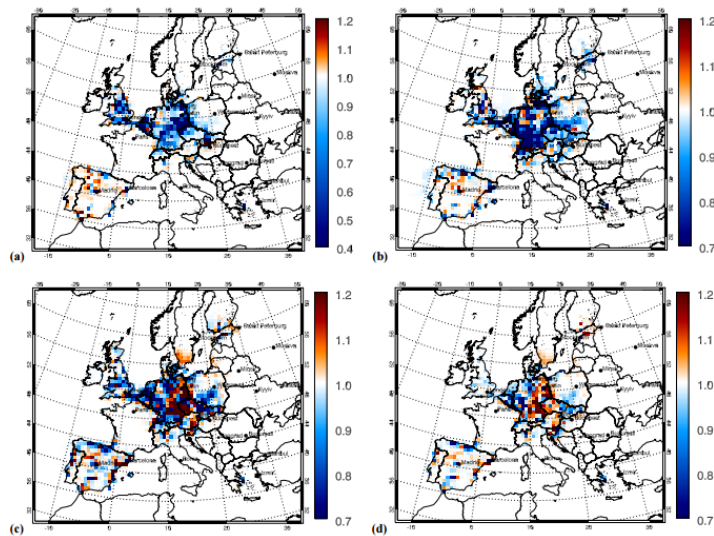


Fig. 10. Emission correction factors for (a) sulfur dioxide, (b) nitrogen dioxide, (c) terminal alkenes, and (d) isoprene at the surface layer, analysed by joint initial value/emission rate optimisation with 24 h assimilation interval placed at 17 August 1997.

4DVAR
Elbern et al,(2007)

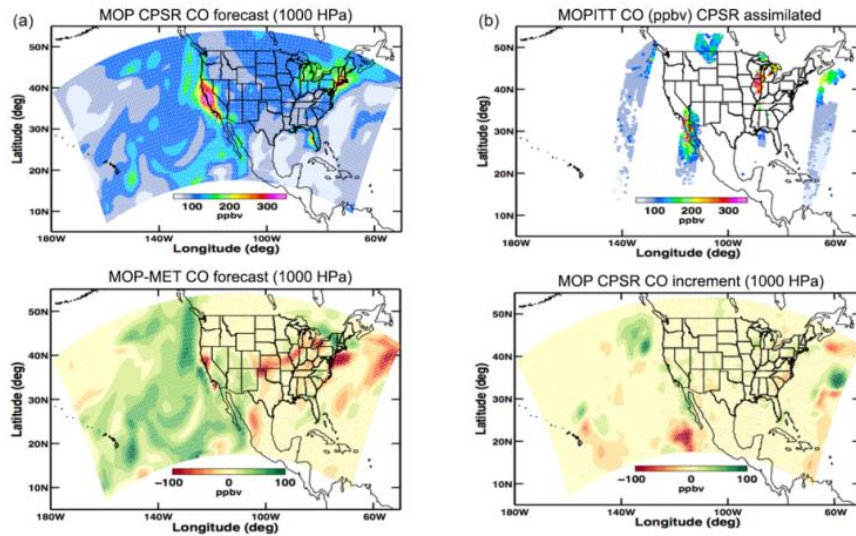


Figure 5. (a) Same as Fig. 1a except for the MOP CPSR experiment and the middle panel from Fig. 1a, the MET DA experiment is not plotted. (b) Same as Fig. 1b except for the MOP CPSR experiment.

EnKF
Mizzi et al,(2016)

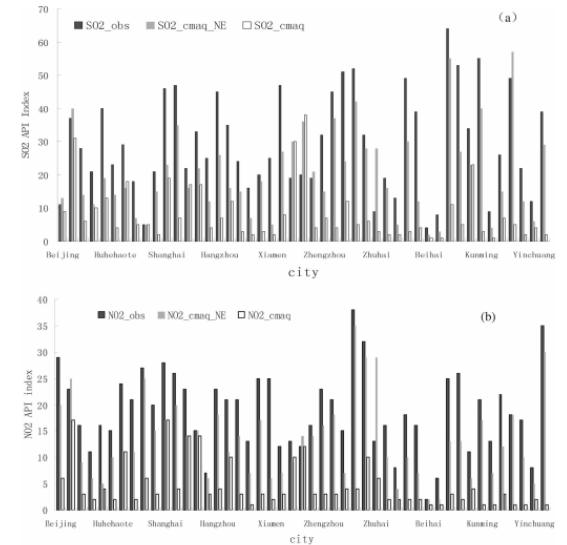


FIG. 2. Comparison of the 1–25 August mean SO₂ and NO₂ API values among the control experiment, nudging experiment, and the observations for the (a) SO₂ API and (b) NO₂ API. The APIs are computed for all 47 cities. It is obvious that the NO₂ and the SO₂ API values from the nudging experiment (light shade) are closer to the observations (dark shade) than are those from the control experiment (white) in nearly all cities.

Nudging
Cheng et al. (2008)



Machine learning

- Machine learning can improve the air quality forecasting accuracy significantly.
- Machine learning can deal with the nonlinear problem.
- In most cases, the effect of machine learning is increased with the growth of database.

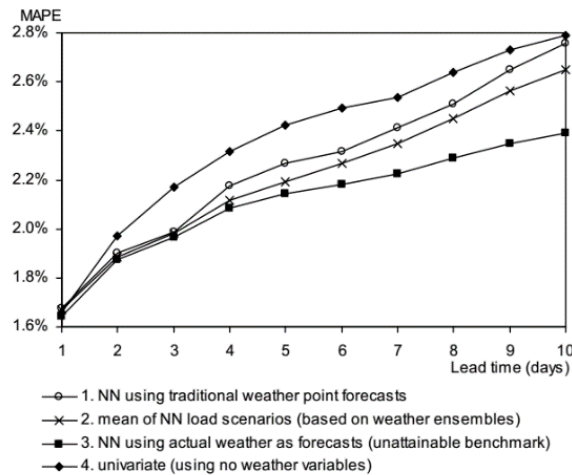


Fig. 3. MAPE for load point forecasts for post-sample period 1 November 1998 to 30 June 2000.

Taylor et al.,(2002). IEEE Transactions on Power Systems.

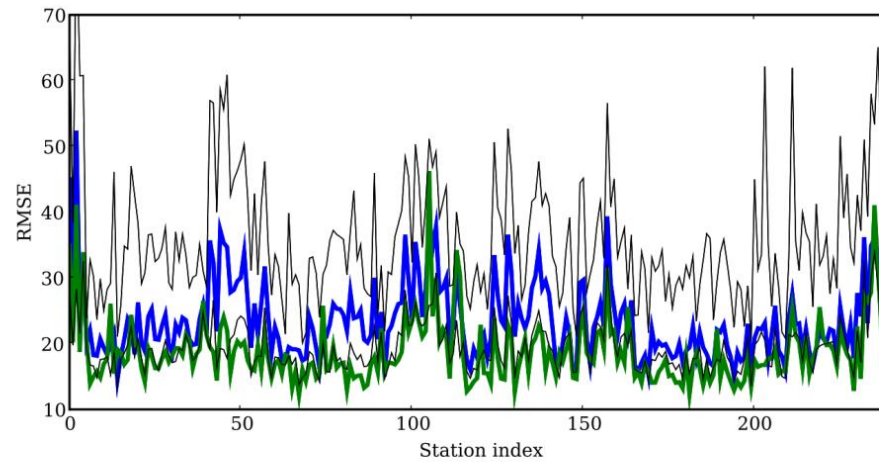


Figure 7. RMSE against the station index (for 241 stations). In green, \bar{R}_{1000} ; in blue, the best model (over all stations); in black, the best model and the worst model for the station.

Mallet, V. et al.,(2009). Journal of Geophysical Research: Atmospheres

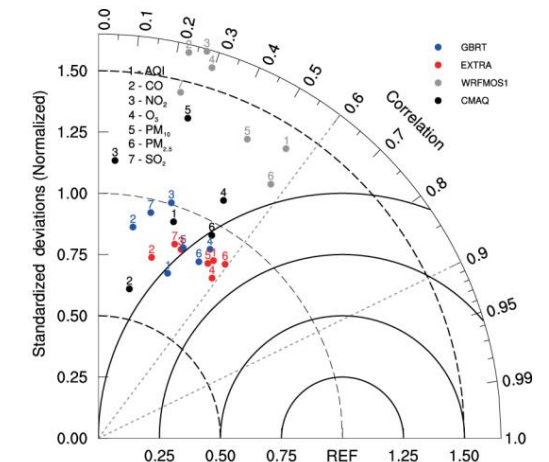


Fig. 4 Taylor diagram of concentrations of six pollutants and AQI from observations and outputs of CMAQ, WRFMOS1, EXTRA and GBRT during 13–24 September, 2016 in HHXC, Xuzhou

Huang. et al.,(2018). Acta Meteorologica Sinica



Contents

- Introduction
- **Data and Methods**
- Results
- Conclusion



Data and Methods

WRFv3.7.1

CMAQv5.3.2

Simulation period: 2 to 30 January in 2019

Resolution: 81km*81km, 27km*27km, 9km*9km

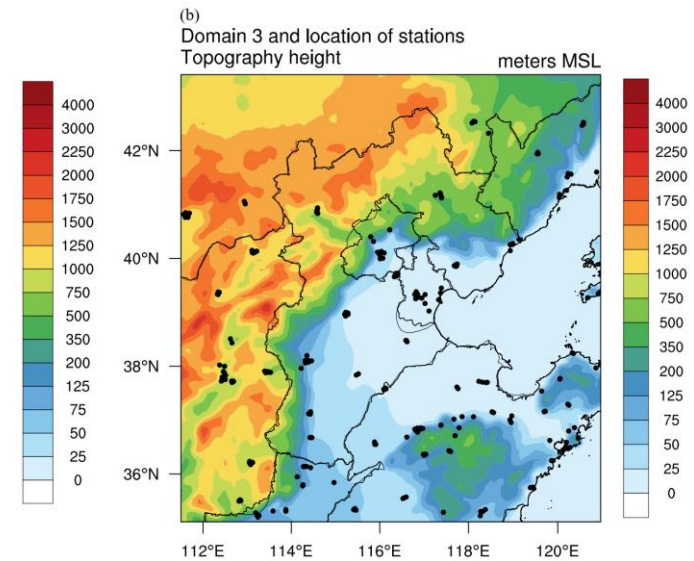
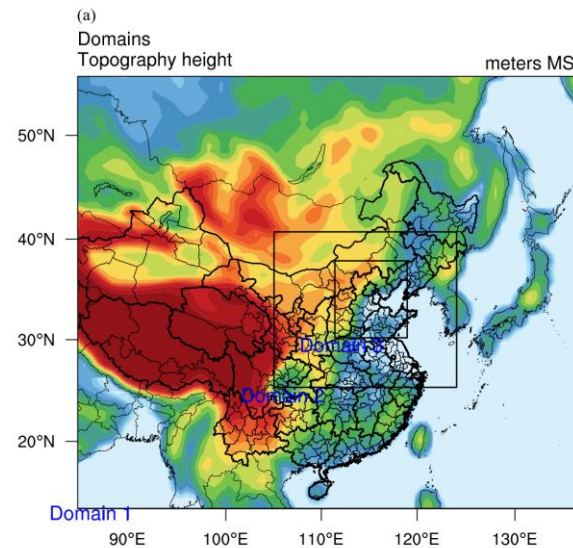
Pollutants: PM_{2.5}, O₃

Observation: PM_{2.5}, O₃ and NO₂ from 255 air quality stations in BTH region

Emission inventory: MEIC 2017

| a. WRFv3.7.1 | | | |
|--|---------------------------------|----------|----------|
| Simulation period | 3–30 January 2019 | | |
| Vertical resolution | 33 vertical levels | | |
| Microphysics scheme | WSM 3-class simple ice scheme | | |
| Boundary layer scheme | YSU scheme | | |
| Surface layer scheme | MM5 scheme | | |
| Land-surface scheme | Unified Noah land-surface model | | |
| Longwave radiation scheme | rrtm scheme | | |
| Shortwave radiation scheme | Dudhia scheme | | |
| Grid-nudging fdda | on | | |
| Domain center | 39.1248°N, 116.5657°E | | |
| Domain id | 1 | 2 | 3 |
| Domain size | 64×75 | 69×81 | 102×96 |
| Starting IJ-indices from the parent domain | × | (30, 19) | (38, 23) |
| Horizontal resolution | 81km | 27 km | 9km |

| a. CMAQv5.3.2 | | | |
|----------------------|--------------|-------|--------|
| Horizontal advection | Yamo | | |
| Vertical advection | WRF | | |
| Horizontal diffusion | Multiscale | | |
| Vertical diffusion | ACM2 | | |
| Deposition | M3Dry | | |
| Chemistry solver | EBI | | |
| Aerosol module | AERO7 | | |
| Cloud module | ACM | | |
| Mechanism | cb6r3_ae7_aq | | |
| Domain id | 1 | 2 | 3 |
| Domain size | 62×73 | 67×79 | 100×94 |





3DVar data assimilation method for initial conditions

$$J(x) = \frac{1}{2}(x - x_b)^T B^{-1}(x - x_b) + \frac{1}{2}(Hx - y)^T R^{-1}(Hx - y) \quad (1)$$

$$J(\delta x) = \frac{1}{2}(\delta x)^T B^{-1}(\delta x) + \frac{1}{2}(H\delta x - d)^T R^{-1}(H\delta x - d) \quad (2)$$

innovation $\delta x = x - x_b$

R : The given measurement instrument error and representative error obtained through spatial allocation

$$\textcircled{1} \quad \varepsilon_R = \gamma \varepsilon_0 \sqrt{\frac{\Delta l}{L}}$$

B : NMC (Error between 24 and 48 hour simulations)

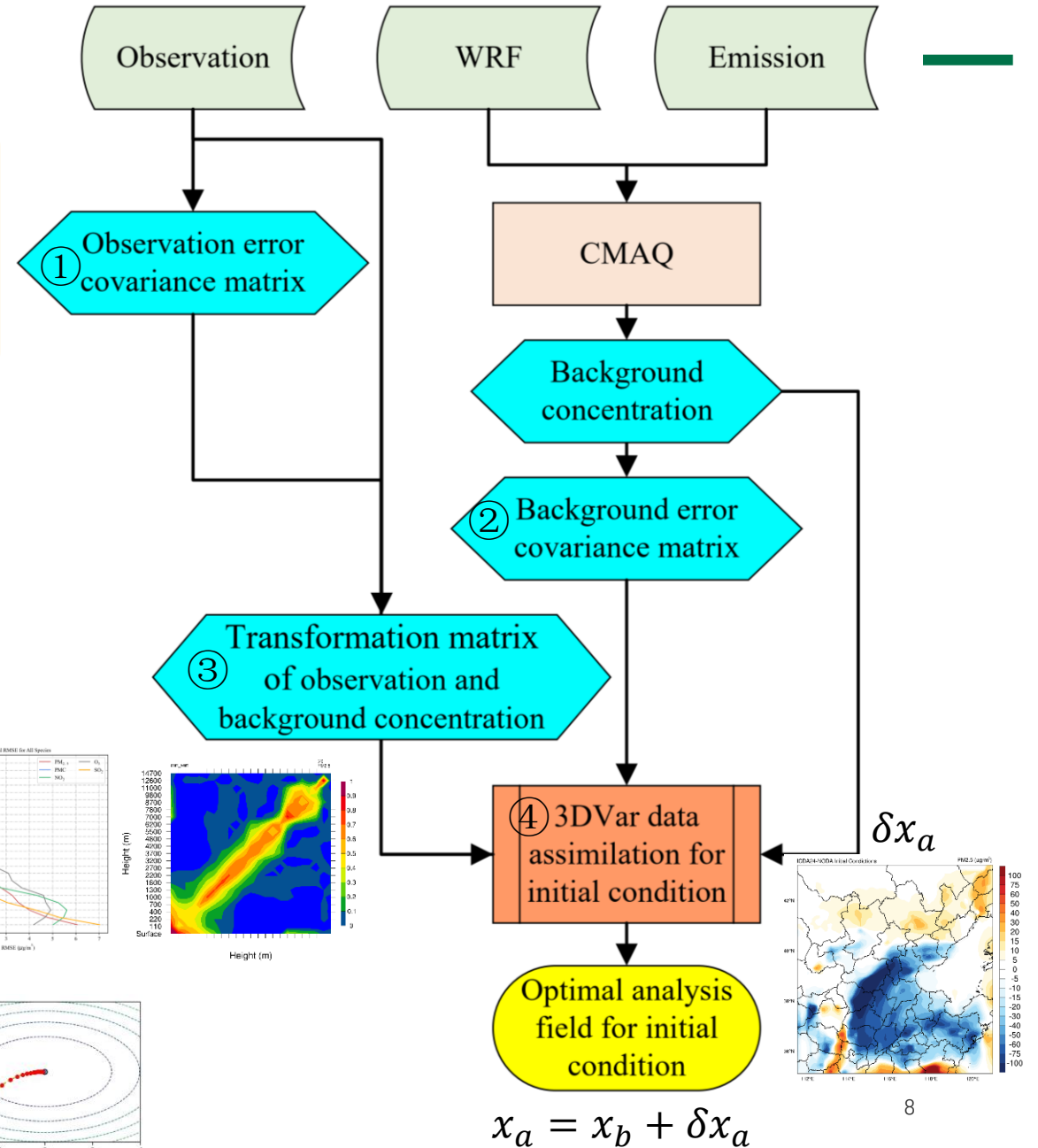
$$\textcircled{2} \quad B = DCD^T; \quad C = C_x \otimes C_y \otimes C_z; \quad \delta x = DC^{\frac{1}{2}}\delta p$$

$$J(\delta p) = \frac{1}{2}(\delta p)^T \delta p + \frac{1}{2}(HDC^{\frac{1}{2}}\delta p - d)^T R^{-1}(HDC^{\frac{1}{2}}\delta p - d)$$

$\textcircled{3}$ H : transformation matrix for linear interpolation of the model field to the location of the observation points

gradient descent method to solve the minimization process
gradient: $\nabla J(\delta x) = B^{-1}(\delta x) + H^T R^{-1}(H\delta x - d)$

$$\textcircled{4} \quad \begin{aligned} \delta x_{k+1} &= \delta x_k + \rho_k S_k \\ S_k &= -\nabla J(\delta x_k) \end{aligned}$$





Extended 3DVar to emission inversion method based on machine learning

From (1): $J(e_t) = \frac{1}{2}(e_t - e_{tb})^T B^{-1}(e_t - e_{tb}) + \frac{1}{2}(H_t^e e_t - y_t)^T R^{-1}(H_t^e e_t - y_t)$ (3)

$$H_t^e = H_t^o S; \quad \delta c_t = H_t^e e_t - H_{tb}^e e_{tb} \approx H_t^{e'}(e_t - e_{tb}) = H_t^{e'} \delta e_t; \quad d_t = y_t - H_{tb}^e e_{tb}$$

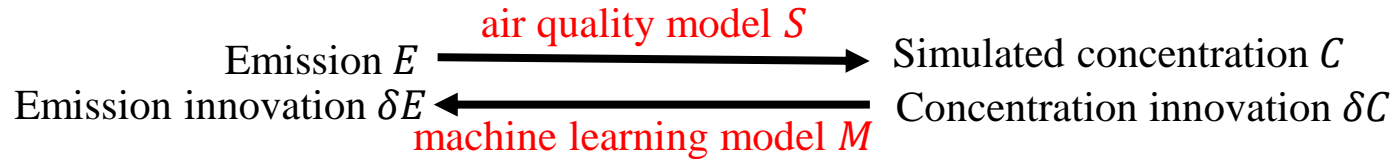
$$J(\delta e_t) = \frac{1}{2}(\delta e_t)^T B^{-1}(\delta e_t) + \frac{1}{2}(H_t^{e'} \delta e_t - d_t)^T R^{-1}(H_t^{e'} \delta e_t - d_t)$$
 (4)

In order to solving the Minimization of $J(\delta e_t)$, S'^T , the tangent linear adjoint mode of air quality model need to be developed, We use machine learning to replace S'^T .

$$H_t^{e'T} = S'^T H_t^{o'T} = M_{\delta c_t} H_t^{o'T}$$

$$\nabla J(\delta e_t) = B^{-1}(\delta e_t) + H_t^{e'T} R^{-1}(H_t^{e'} \delta e_t - d_t) = B^{-1}(\delta e_t) + M_{\delta c_t} H_t^{o'T} R^{-1}(H_t^{o'} \delta c_t - d_t)$$
 (5)

S : air quality model ; H_t^e : the transformation matrix between the emission intensity and the observation



$$\delta C_A = [\delta c_1 \quad \dots \quad \delta c_t]$$

$$\delta E_A = [\delta e_1 \quad \dots \quad \delta e_t]$$

$$\delta E_A = M(\delta C_A)$$

S'^T means δC to δE

$$M \approx S'^T$$

$$H_t^{e'T} \approx M_{\delta c_t} H_t^{o'T}$$

The H^T for δx in 3DVar initial data assimilation Changed to $M_{\delta c_t} H_t^{o'T}$ for δe_t in 3DVar emission inversion combined with machine learning.

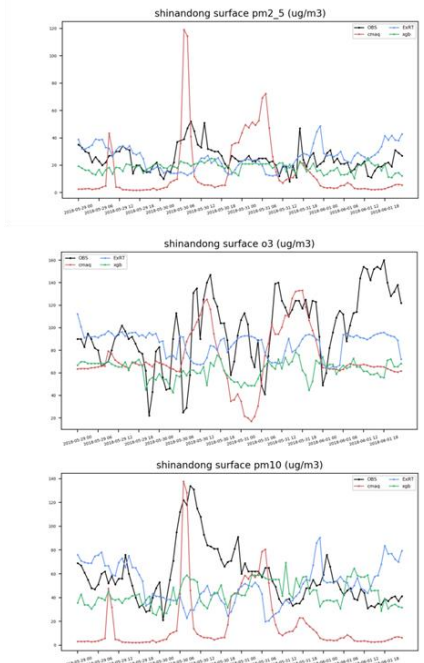
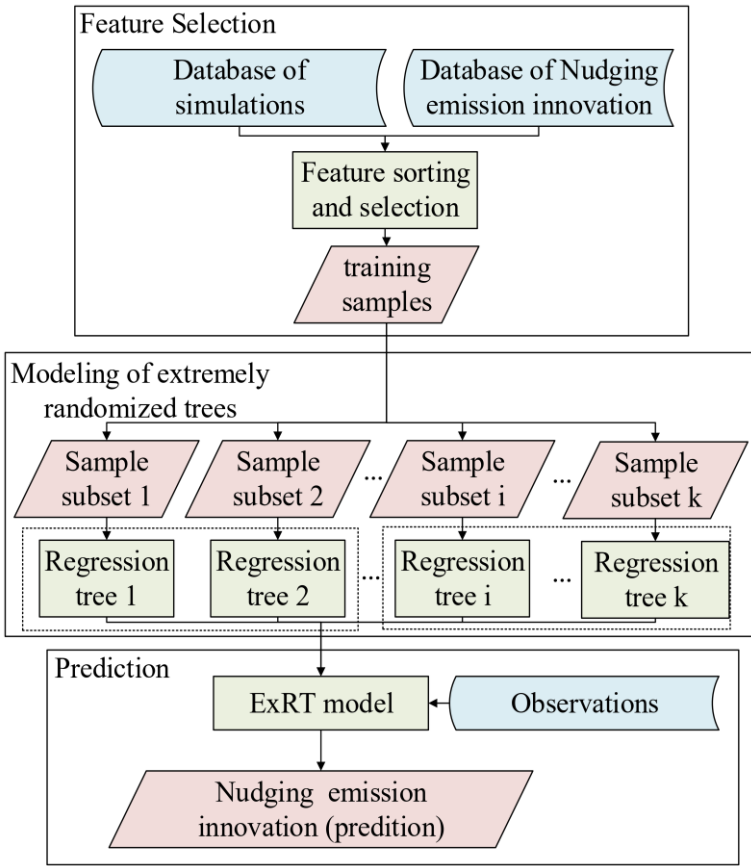
δC_A : All the simulated concentration innovation in database

δE_A : Emission innovation in one-to-one correspondence with δC_A

M : machine learning model



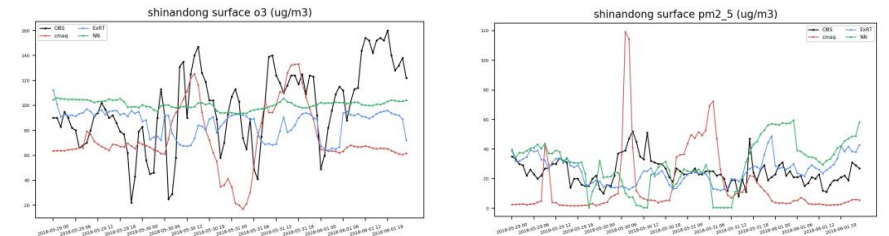
Why Extremely Random Trees?



1.The comparison of ExRT and XGBoost in WRFChem-MOS in Qingdao

2.The comparison of ExRT、GBRT and Adaboost in CMAQ-MOS in Qingdao

| | RMSE | SO ₂ | NO ₂ | PM ₁₀ | CO | O ₃ | PM _{2.5} |
|-----------|------|-----------------|-----------------|------------------|------|----------------|-------------------|
| CMAQ | | 106.23 | 59.84 | 137.85 | 0.36 | 34.28 | 105.45 |
| MOS_EXTRA | | 14.04 | 19.06 | 48.06 | 0.21 | 44.65 | 23.00 |
| MOS_GBRT | | 15.85 | 19.26 | 48.85 | 0.21 | 44.45 | 21.58 |
| MOS_ADA | | 13.91 | 19.81 | 50.24 | 0.21 | 47.55 | 23.03 |

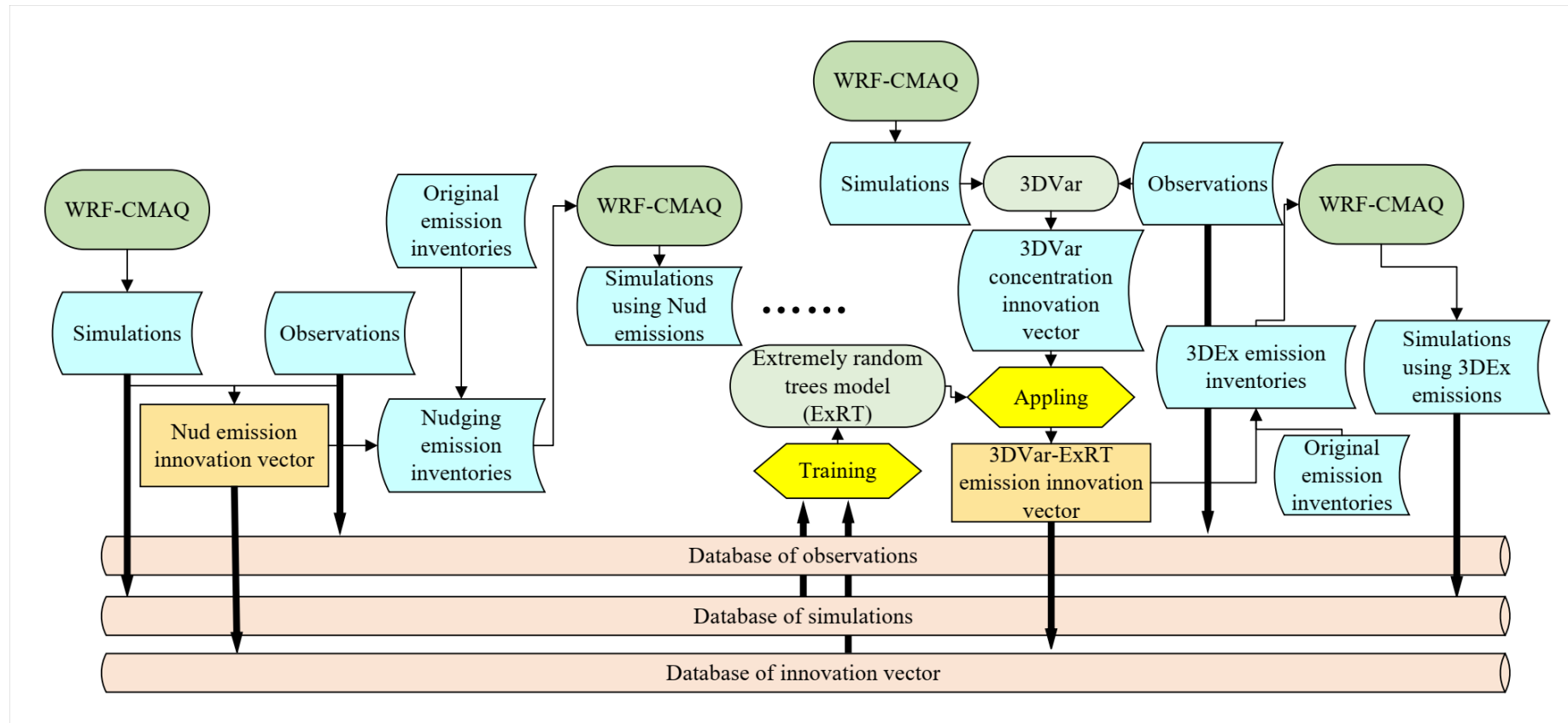


3.The comparison of ExRT and BPNN in CMAQ-MOS in Qingdao

ExRT has been proved to be a stable and efficient method comparing to other methods in our previous studies in improving air quality forecasting accuracy using model output statistics method.



Framework of the 3DVar-ExRT method



- Nudging method was used to create the basic database of simulations and innovations, using simulations of CMAQ and the ground-based observations.
- These data are employed to train a machine learning model using extremely random trees method (ExRT), and to store the relations between innovation vector and simulations in the trees.



The emission data assimilation in operational forecast of CMAQ

- Using Nudging method to calculate the hourly emission innovation vector from 2 to 14 January, 2019 and create the database of observation, simulation and innovation vector . The model restart every 24 hours and store the data of observation, simulation and innovation vector in the database.
- Using Nudging (Nud) and 3DVar-ExRT (3DEx) method to adjust anthropogenic emissions of PM_{2.5}, VOCs and NO_x from 15 to 30 January,2019.
- Every 24 hours, all the simulation of PM_{2.5}, O₃ and NO₂ and innovation vector of PM_{2.5}, VOC and NO_x data in the database was used to train the PM_{2.5} and VOCs machine learning model.
- We use the machine learning model and 72h observation before model restart to get the 3DEx innovation vector for the next day.
- Notice:NO₂ observations and simulation was used to calculate the emission of NO_x
O₃ observations and simulation was used to calculate the emission of VOCs in Nud
O₃ and NO₂ observations and simulation was used to calculate the emission of VOCs in 3DEx



Contents

- Introduction
- Data and Methods
- **Results**
- Conclusion



Daily change of PM_{2.5}, VOC and NO_x emission inventories

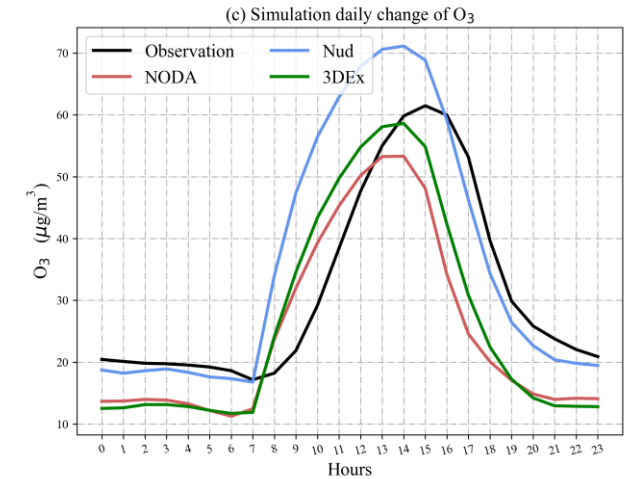
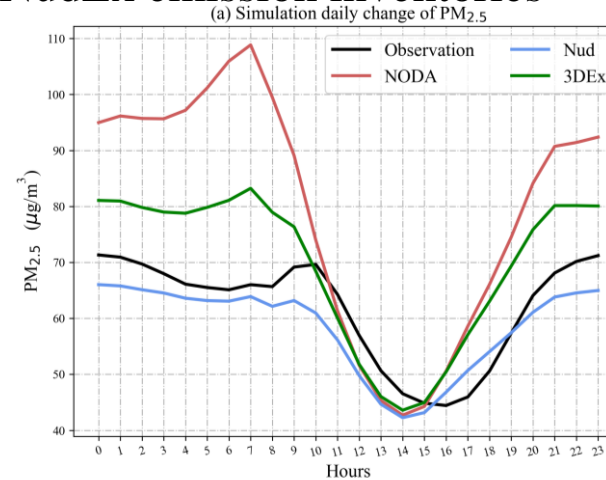
NO₂ simulations, observations and NO_x emission inventories was used in the ExRT model to calculate the 3DEx innovation vector of NO_x.

O₃ and NO₂ simulations, observations and VOC emission inventories was used in the ExRT model to calculate the 3DEx innovation vector of VOCs.

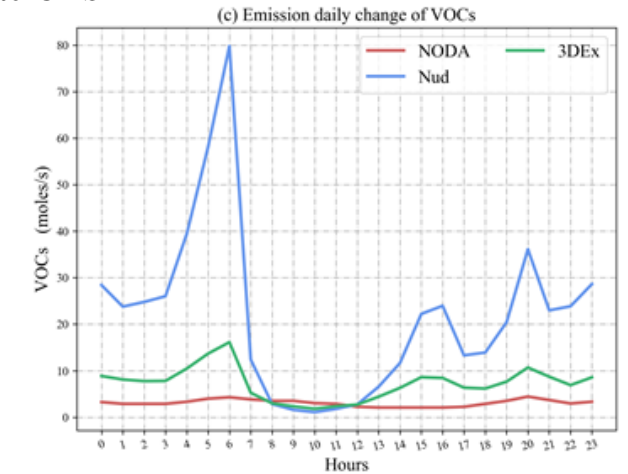
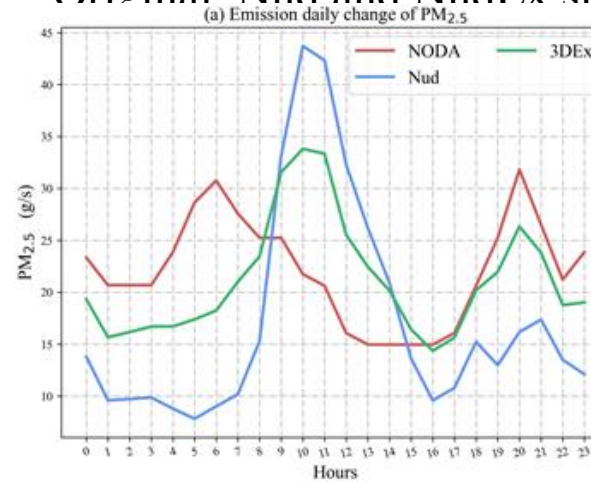
Nud method can only consider direct reaction between O₃ and VOCs
 3DEx can consider all direct and indirect reactions into the nonlinear ExRT model

- 1 NO₂ + hv + O₂ → O₃ + NO
- 2 NO + O₃ → NO₂ + O₂
- 3 RH + OH + O₂ → RO₂ + H₂O
- 4 HO₂ + NO → OH + NO₂
- 5 RO₂ + NO + O₂ → φ · HO₂ + φ · R'CHO + φ · NO₂ + (1 - φ) · RONO₂
- 6 O₃ + hv + H₂O → 2 · OH + O₂
- 7 O₃ + OLE → products
- 8 O₃ + OH → HO₂ + O₂
- 9 O₃ + HO₂ → OH + 2 · O₂
- 10 NO₂ + OH → HNO₃

Simulation Daily Change of PM_{2.5}, O₃ using Original, Nud and NudEx emission inventories



Emission Daily Change of PM_{2.5}, VOCs emission inventories in Original Nud and NudEx simulations



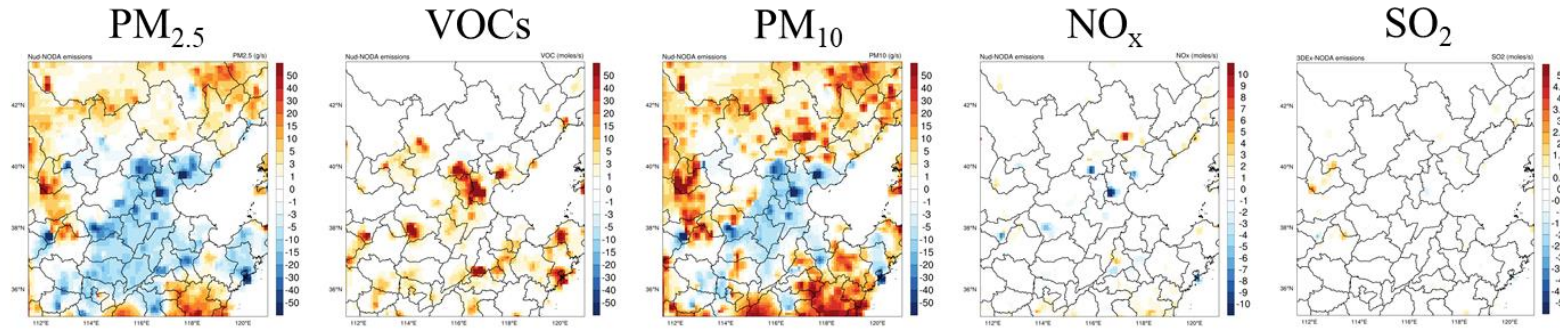


The emission changes before and after emission inversion

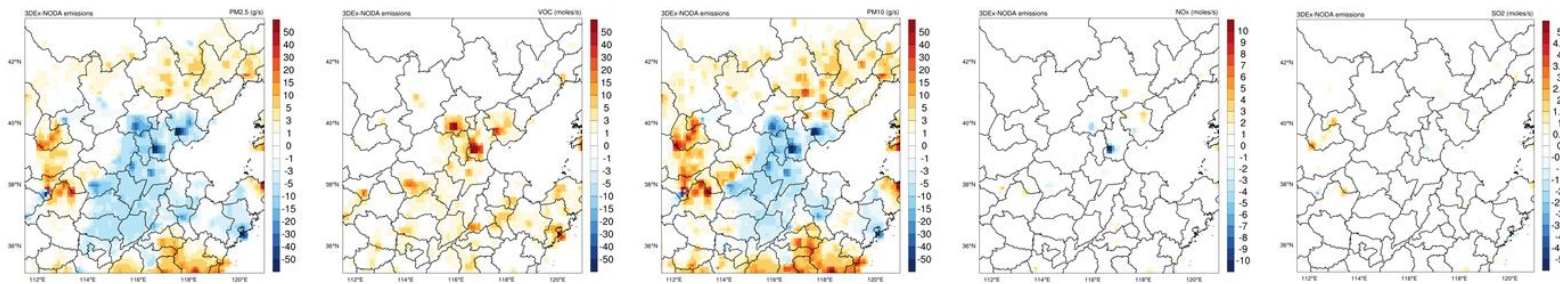
Simulation time:
2019.1.15 to 2019.1.30

- MEIC has time lag and cannot reflect the current emissions.
- There has been improvement in the inversion, with a significant decrease in PM_{2.5} and a significant increase in VOCs.

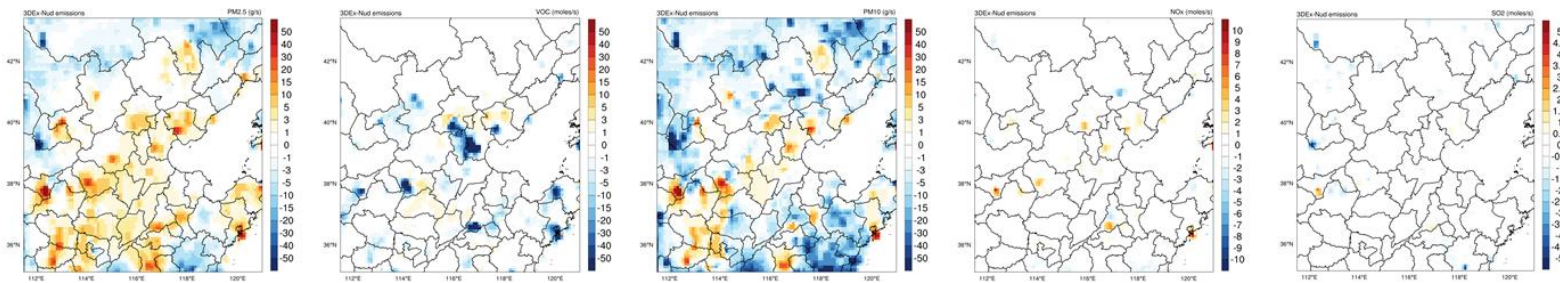
Nud-NODA



3DEx-NODA



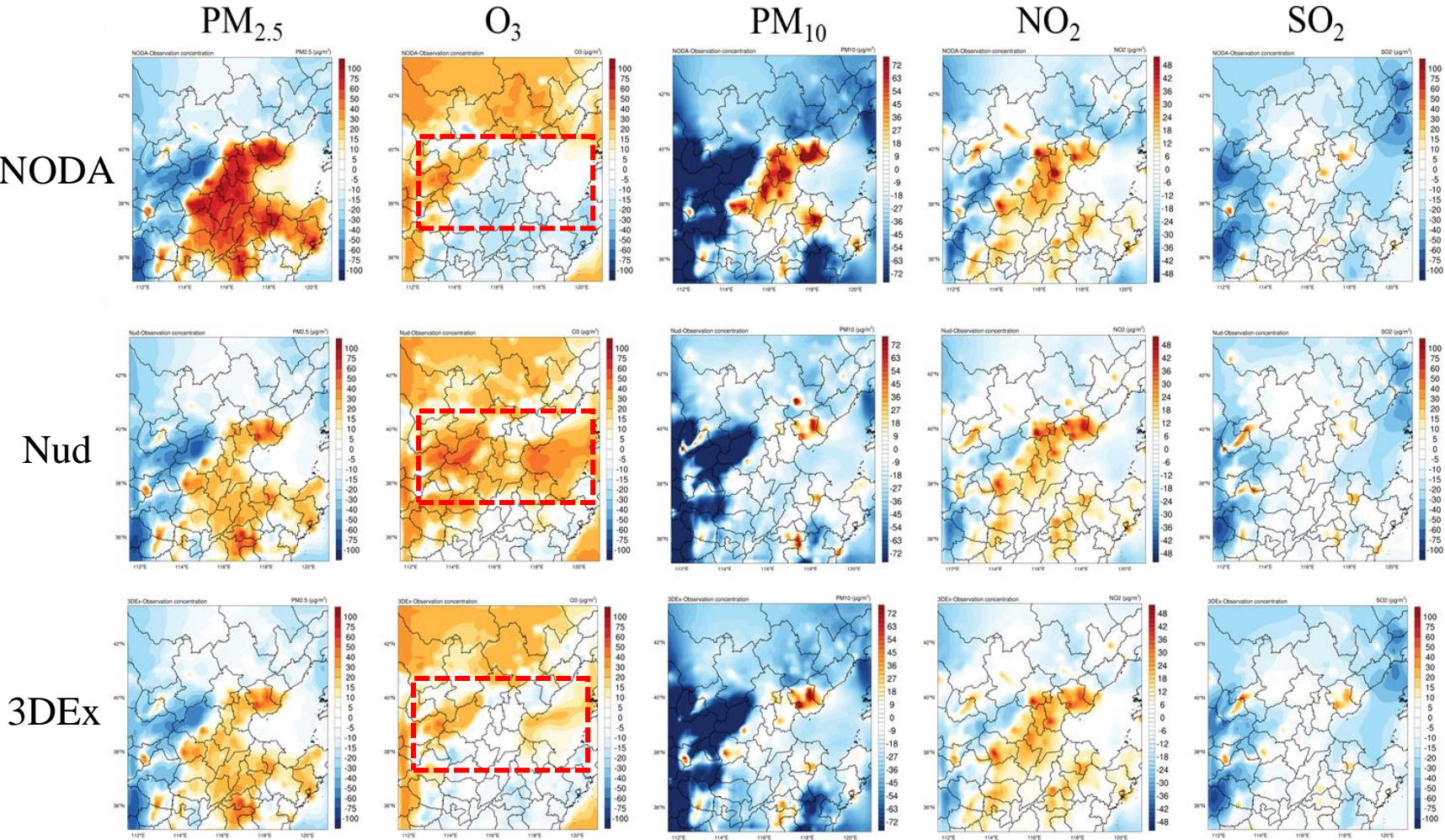
3DEx-Nud



The 2019 emission inventory = original emission inventory (MEIC 2017) + **emission innovation** (inversed by using the 2019 observations)



Results of emission inversion



The Nudging method cannot handle nonlinear problems, attributing all O₃ errors to the underestimation of VOCs, and the inversion of O₃ actually deteriorates.

3DEx: O₃-NO_x-VOCs nonlinear processes ≈ O₃, NO₂ concentration innovation + VOCs, NO_x emission innovation + ExRT model

$$\begin{aligned}\delta E_{NOx} &= M(\delta C_{O3}, \delta C_{NO2}) \\ \delta E_{VOCs} &= M(\delta C_{O3}, \delta C_{NO2}, \delta E_{NOx})\end{aligned}$$

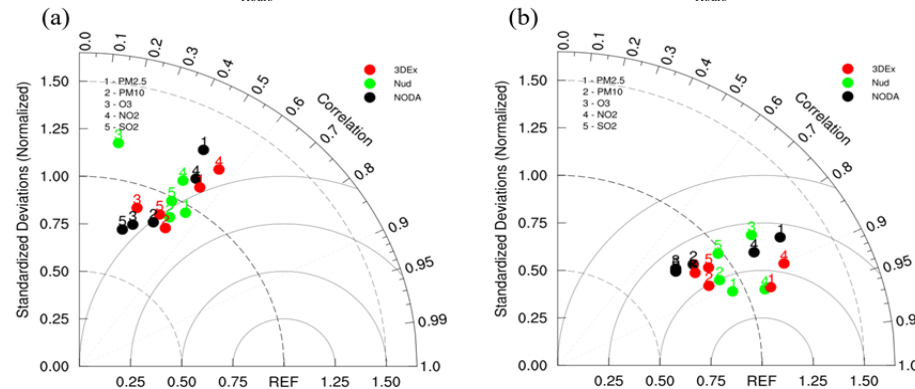
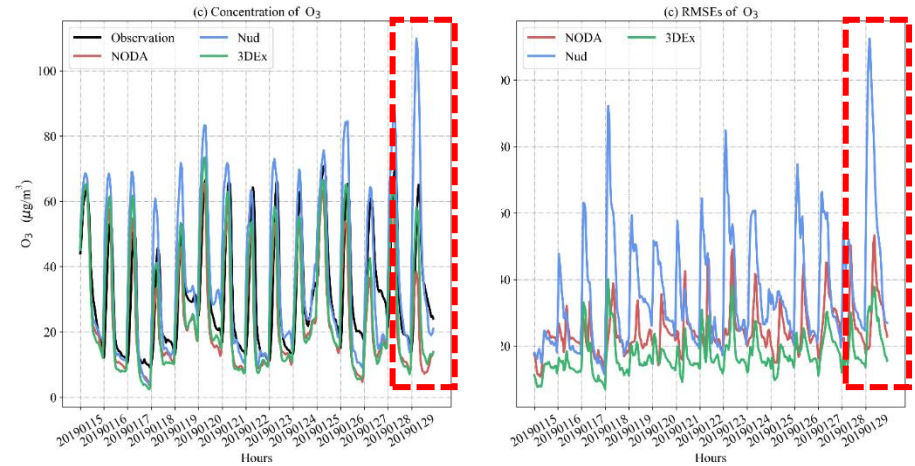
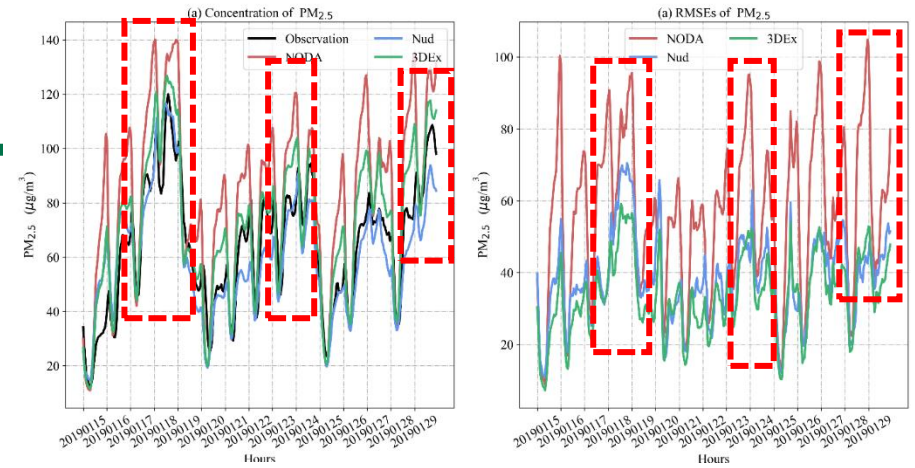
3DEx can significantly improve the simulation of O₃.



Assessment of the 3DEx emission inversion method

As for $PM_{2.5}$, Nud can significantly improve the forecasting accuracy and 3DEx was better.

As for O_3 , Nud reckon without nonlinear reactions of O_3 -Nox-VOC made the forecasting worse. But 3DEx can partly take the place of the nonlinear reactions and had a better performance.



| | $PM_{2.5}$ | | | O_3 | | |
|--|------------|--------------|--------------|-------------|-------|--------------|
| | NODA | Nud | 3DEx | NODA | Nud | 3DEx |
| \overline{Rs} | 0.47 | 0.54 | 0.54 | 0.33 | 0.16 | 0.32 |
| \overline{RMSEs} ($\mu\text{g}/\text{m}^3$) | 56.44 | 38.23 | 33.82 | 24.60 | 36.61 | 17.58 |
| Ra | 0.85 | 0.91 | 0.93 | 0.75 | 0.81 | 0.81 |
| \overline{RMSEa} ($\mu\text{g}/\text{m}^3$) | 24.41 | 10.59 | 12.45 | 13.91 | 14.86 | 12.49 |

● 3DEx-NODA $PM_{2.5}$: **RMSEs 40%** **RMSEa 49%**

O_3 : **RMSEs 29%** **RMSEa 10%**

\overline{Rs} : the hourly averaged spatial correlation coefficient

\overline{RMSEs} : the hourly averaged spatial root mean squared error

Ra : the correlation coefficient of the site averaged concentration

\overline{RMSEa} : the root mean squared error of the site averaged concentration



Contents

- Introduction
- Data and Methods
- Results
- Conclusion



Conclusion

- This efficiently and extensibility framework of 3DVar-ExRT method has been proved to be a good way to adjust anthropogenic emissions.
- 3DVar-ExRT method can improve the $PM_{2.5}$ and O_3 forecasting accuracy and the optimization was better with the growth of database.
- The iterations can be done with the operational forecast, which means the computing resources can be greatly reduced using this method.
- Both linear and nonlinear emission sources can be optimized using 3DVar-ExRT methods.



Thank You!

Email: congwhuang@hubu.edu.cn



WeChat

